Applying a New Trigonometric Radial Basis Function Approximation in Solving Nonlinear Vibration Problems

Hossein Talebi Rostami (Talebirostami92@gmail.com)
Amirkabir University of Technology
Maryam Fallah Najafabadi
Babol Noshirvani University of Technology
Davood Domiri Ganji
Babol Noshirvani University of Technology

Research Article

Keywords: RBF method, Semi-analytical approach, Nonlinear equations, Vibration problems, Oscillation parameters

Posted Date: August 15th, 2023

DOI: https://doi.org/10.21203/rs.3.rs-3258099/v1

Applying a New Trigonometric Radial Basis Function Approximation in Solving Nonlinear Vibration Problems

Hossein Talebi Rostami[a,*], Maryam Fallah Najafabadi[b], Davood Domiri Ganji[b]

[a] Department of Mechanical Engineering, Amirkabir University of Technology, Tehran, Iran

[b] Department of Mechanical Engineering, Noshirvani University of Technology, Babol, Iran

*Corresponding author's Email: Talebirostami92@gmail.com

Abstract

This study introduces a semi-analytical New Trigonometric Radial Basis Function (NTRBF) method for solving strongly nonlinear differential equations in vibration problems. The method uses a particular trigonometric function to deal with differential equations in an extraordinary and original approach. It was compared to four different problems, including the Global Residue Harmonic Balance Method (GRHBM) in solving circular sector oscillator problem, the Continuous Piecewise Linearization method (CPLM) in solving strong nonlinear differential equation of a tapered beam, the Differential Transform Method (DTM) to solve centrifugal rotating frame motion, and Akbari-Ganji's Method (AGM) to solve Duffing-type nonlinear oscillator. These problems were solved in different conditions. The plots and tables represent both cumulative and maximum errors between the NTRBF and other methods, which use the numerical 4th-order Runge-Kutta method as a benchmark for accuracy. The outcomes prove the high accuracy and efficiency of the innovative technique and its unique capability in solving various nonlinear vibration problems.

Keywords: RBF method; Semi-analytical approach; Nonlinear equations; Vibration problems; Oscillation parameters;

1. Introduction

Scientists have always been looking for new methods to solve mathematical problems with no answer or improve the solution that has already been achieved. These improvements can be in the shape of higher accuracy, less computation time, etc. [1], [2], [3]. The radial basis function (RBF) method is a powerful method for solving differential equations related to many physical problems [4], [5], [6]. Radial basis functions are a type of function whose value depends only

on the distance between a point and the origin. Linear combinations of these functions can bring us the solution for many ordinary or partial differential equations with strong nonlinearity. The most significant merits of the RBF method are accuracy and convergence power. Even though the RBF method has many advantages, it is impossible to apply RBF approximation to all differential problems. Nevertheless, many modifications have been made to increase the efficiency and accuracy of the RBF method; for instance: Liu et al. [7] invented a multiple-scale multiquadric RBF for solving elliptic PDEs and the related inverse Cauchy problems. The results showed that the technique was precise and stable against large noises. Sun et al. [8] improved the ordinary RBF to a local radial basis function meshless method for solving the heat transfer problem with radiation. In that paper, the RBF was compounded to a polynomial basis to form the approximating function, so meshes were not needed. The proposed function was more effective, with outstanding stability for solving the radiative problems. Jankowska et al. [9] applied the Kansa-RBF method to two dimensions boundary value problems. They solved some numerical examples to indicate the accuracy and efficiency of the method. Shankar et al. [10] used RBF to solve the 2D problem of the surfaces. They used the least orthogonal interpolation for the functions. The method was free of stagnation errors and showed high orders of convergence. In the research of Li et al. [11], a new hybrid scheme based on the multiquadric RBF-FD method was proposed to solve the convection-dominated diffusion problems. The numerical outcomes illustrated that the new scheme has an advantage over the standard scheme in feasibility and correction. Zhang [12] created a precise RBF method for solving partial differential equations. The novel method, coupled radial basis function, was not dependent on shaping parameters–two examples in the paper proved the method's robustness. Bhardwaj and Kumar [13] found a new solution for the time–fractional Tricomi-type equations based on the RBF meshless method. They evidenced that the proposed method was practicable and stable for all problem conditions. Reutsky and Lin [14] applied an innovative RBF method for an anisotropic inhomogeneous medium for 3D convection-diffusion-reaction problems. Several examples demonstrated the high effectiveness of the method in single and double-connected domains. Aràndiga et al. [15] applied a multiquadric radial basis function to examine tactics to rebuild discontinuous one-dimensional functions for indicating the shape parameter of the RBF. They presented numerical examples to validate their study. Ullah [16] searched for a solution for high-dimensional Black–Scholes partial differential equations. He used the radial basis function-finite difference method in the multiquadric form and demonstrated its efficiency and precision. Qiao et al. [17] invented a fast finite difference/RBF meshless technique for time-fractional convection-diffusion

problems. The method was so effective for complicated boundaries and regions and lessened the calculation time while increasing accuracy. Mai-Duy and Strunin [18] used the integral radial basis function to solve the second-order nonlinear differential equation by a new compressed approximation scheme. The outcomes showed great convergence of the offered method. Ma et al. [19] presented a new Kansa method with the fictitious center approach in which polynomial basis functions amplify the radial basis function (RBF) approximation. Once again, the shape parameter dependency was eliminated in the article to improve the accuracy and stability. Zeng and Zhu [20] invented an RBF-based method with application in implicit surface reconstruction. The technique unifies both interpolation and approximation of the RBFs. Moreover, the outcomes show that the method is precision-controlled and rapid. Ang [21] found a numerical solution for Cattaneo–Vernotte hyperbolic equation using the RBF approximation. Several equations were solved to confirm the validness and precision of the presented solution. Wu et al. [22] proposed a new RBF that integrates multi-dimensional scaling for carbon decrease in industries. They assessed the outcomes and the real data and proved the technique's efficiency and reliability. Some other significant researches in the literature are presented in [23], [24], [25], [26], [27], [28].

This research introduces an original technique, namely a new trigonometric radial basis function for solving strongly nonlinear differential equations with application in vibration problems. The method uses a unique trigonometric function with inherent oscillatory features to fill the gap in solving differential equations related to vibrations. Compared to all other radial basis functions, improvements in this technique result in less significant maximum and average errors, higher accuracy and convergence, and high adaptability to multifarious vibration problems. In order to prove the method's spectacular properties, we explained the process of solution and solved four distinct vibration problems from the literature. Then we compared the outcomes with the previous methods and used a numerical method to benchmark accuracy.

2. New Trigonometric Radial Basis Function Approximation

Approximation for solving vibration problems is possible through a wide range of radial basis functions; however, our choices are restricted by the problem's inherent characteristics. For example, multiquadric functions are a proper choice for velocity in fluid mechanics, whereas it is not suitable for displacement in harmonic oscillation problems. Table 1 shows the popular radial basis functions. Here we introduce a new trigonometric radial basis function (NTRBF) for solving nonlinear vibration problems. This novel function is $\sin(\varepsilon^2(x-C)^2)$, in which

$x-C$ represents the distance between the input x and some fixed point C and ε is the shape parameter. Fig. 1. shows the graph of the mentioned function in three different shape parameters and when the fixed point is considered the origin $(C=0)$.

Table 1 List of common radial basis functions [29], [30]

Name	**Function**
Gaussian	$\exp(-\varepsilon^2(x-C)^2)$
Multiquadric	$\sqrt{1+\varepsilon^2(x-C)^2}$
Inverse Multiquadric	$1/\sqrt{1+\varepsilon^2(x-C)^2}$
Inverse Quadratic	$1/(1+\varepsilon^2(x-C)^2)$
Generalized Multiquadric	$(1+\varepsilon^2(x-C)^2)^{\beta}, \quad \beta \in \sim$
Laguerre–Gaussian	$(2-\varepsilon^2(x-C)^2)\cdot\exp(-\varepsilon^2(x-C)^2)$
Poisson	$\sqrt{\frac{2}{\pi}}\cdot\frac{\sin(\varepsilon(x-C))}{\varepsilon(x-C)}$
Radial Power	$(\varepsilon(x-C))^{\beta}, \quad 0<\beta\notin 2$
Thin Plate spline	$(\varepsilon(x-C))^{2\beta}\cdot\log(\varepsilon(x-C)), \quad \beta\in$
Wendland	$(1-\varepsilon(x-C))^6+(35\varepsilon^2(x-C)^2+18\varepsilon(x-C)+3)$
Gneiting	$(1-\varepsilon(x-C))^5+(-27\varepsilon^2(x-C)^2+5\varepsilon(x-C)+1)$
Hyperbolic Secant	$2/(\exp(\varepsilon(x-C))+\exp(-\varepsilon(x-C)))$

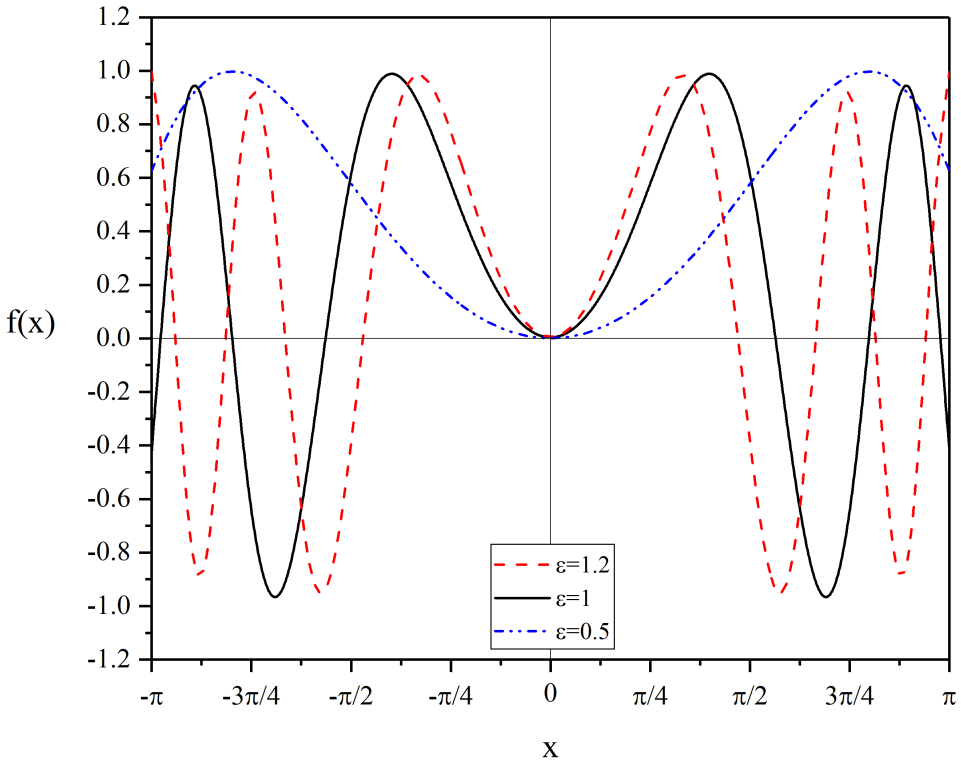

Fig. 1 Graph of new trigonometric radial basis function in different shape parameters

Symmetry, oscillatory form, and high dependence on shape parameters are prominent features in the new trigonometric RBF plot. Unlike the other common RBFs, these features make it an excellent choice for vibration problems. In general, the procedure of solving a problem via the new trigonometric radial basis function is slightly different from solving a problem with the usual RBF [30]. In the first step, we introduce a set of finite points (C) called center or origin $(C \in \sim)$. The value of each center in the primary function is real– $g(C) \in \sim$. The goal is to approximate an unknown function at those points. For a set of n differential equations with n unknown functions (or it can be just one differential equation with one unknown function), we have:

$$DE_i : f_i\left(g(x), g'(x), ..., g^{(j)}(x), h(x), h'(x), ..., h^{(k)}(x), ...\right) = 0, \qquad i = 1, ..., n \tag{1}$$

The corresponding initial or boundary conditions are:

$$
\begin{aligned}
&g(0)=g_0,\quad g(L)=g_{L0},\\
&g'(0)=g_1,\quad g'(L)=g_{L1},\\
&\vdots\\
&g^{(j-1)}(0)=g_{j-1},\quad g^{(j-1)}(L)=g_{L(j-1)},\\
&h(0)=h_0,\quad h(L)=h_{L0},\\
&h'(0)=h_1,\quad h'(L)=h_{L1},\\
&\vdots\\
&h^{(k-1)}(0)=h_{k-1},\quad h^{(k-1)}(L)=h_{L(k-1)},\\
&\vdots
\end{aligned}
\tag{2}
$$

We form a series of new trigonometric radial basis functions based on differential equations to approximate the main functions. The series can have any number of sentences with a value between one to infinity based on convergence, precision, and calculation time.

$$
\begin{aligned}
&g(x)=\sum_{p=1}^{m}A_pG_p(x),\qquad 1\le m<\infty.\\
&h(x)=\sum_{q=1}^{s}B_qH_q(x),\qquad 1\le s<\infty.\\
&\text{M}
\end{aligned}
\tag{3}
$$

G_p, H_q are new trigonometric radial basis functions, and A_p, B_q are the corresponding real coefficients $(A_p, B_q \in \sim)$. A more expanded form of Eq. (3) is:

$$
\begin{aligned}
&g(x)=\sum_{p=1}^{m}A_p\cdot\sin(\varepsilon_g^2(x-C_{gp})^2),\qquad 1\le m<\infty.\\
&h(x)=\sum_{q=1}^{s}B_q\cdot\sin(\varepsilon_h^2(x-C_{hq})^2),\qquad 1\le s<\infty.\\
&\text{M}
\end{aligned}
\tag{4}
$$

$\varepsilon_g, \varepsilon_h$ are the shape parameters of radial basis functions for adjusting the intensity of inlet values, and C_p, C_q are centers. Centers, shape parameters, and the number of sentences in the series are three levers to regulate the series. Based on the presented series, $g(x), h(x)$ and their derivatives are:

$$g(x) = A_1 \sin(\varepsilon_g^2 (x - C_{g1})^2) + A_2 \sin(\varepsilon_g^2 (x - C_{g2})^2) + ... + A_m \sin(\varepsilon_g^2 (x - C_{gm})^2),$$
$$g'(x) = 2A_1 \varepsilon_g^2 (x - C_{g1}) \cdot \cos(\varepsilon_g^2 (x - C_{g1})^2) + 2A_2 \varepsilon_g^2 (x - C_{g2}) \cos(\varepsilon_g^2 (x - C_{g2})^2) + ...$$
$$+2A_m \varepsilon_g^2 (x - C_{gm}) \cos(\varepsilon_g^2 (x - C_{gm})^2),$$
M
$$g^{(j)}(x) = A_1 G_1^{(j)}(x) + A_2 G_2^{(j)}(x) + ... + A_m G_m^{(j)}(x).$$

$$h(x) = B_1 \sin(\varepsilon_h^2 (x - C_{h1})^2) + B_2 \sin(\varepsilon_h^2 (x - C_{h2})^2) + ... + B_s \sin(\varepsilon_h^2 (x - C_{hs})^2), \quad (5)$$
$$h'(x) = 2B_1 \varepsilon_h^2 (x - C_{h1}) \cdot \cos(\varepsilon_h^2 (x - C_{h1})^2) + 2B_2 \varepsilon_h^2 (x - C_{h2}) \cos(\varepsilon_h^2 (x - C_{h2})^2) + ...$$
$$+2B_s \varepsilon_h^2 (x - C_{hs}) \cos(\varepsilon_h^2 (x - C_{hs})^2),$$
M
$$h^{(k)}(x) = B_1 H_1^{(k)}(x) + B_2 H_2^{(k)}(x) + ... + B_s H_s^{(k)}(x).$$
M

In $x = 0$, the following sentences are formed:

$$g(0) = g_0 = A_1 \sin(\varepsilon_g^2 (-C_{g1})^2) + A_2 \sin(\varepsilon_g^2 (-C_{g2})^2) + ... + A_m \sin(\varepsilon_g^2 (-C_{gm})^2),$$
$$g'(0) = g_1 = 2A_1 \varepsilon_g^2 (-C_{g1}) \cdot \cos(\varepsilon_g^2 (-C_{g1})^2) + 2A_2 \varepsilon_g^2 (-C_{g2}) \cos(\varepsilon_g^2 (-C_{g2})^2) + ...$$
$$+2A_m \varepsilon_g^2 (-C_{gm}) \cos(\varepsilon_g^2 (-C_{gm})^2),$$
M
M
$$g^{(j-1)}(0) = g_{j-1} = A_1 G_1^{(j-1)}(0) + A_2 G_2^{(j-1)}(0) + ... + A_m G_m^{(j-1)}(0).$$

$$h(0) = h_0 = B_1 \sin(\varepsilon_h^2 (-C_{h1})^2) + B_2 \sin(\varepsilon_h^2 (-C_{h2})^2) + ... + B_s \sin(\varepsilon_h^2 (-C_{hs})^2), \quad (6)$$
$$h'(0) = h_1 = 2B_1 \varepsilon_h^2 (-C_{h1}) \cdot \cos(\varepsilon_h^2 (-C_{h1})^2) + 2B_2 \varepsilon_h^2 (-C_{h2}) \cos(\varepsilon_h^2 (-C_{h2})^2) + ...$$
$$+2B_s \varepsilon_h^2 (-C_{hs}) \cos(\varepsilon_h^2 (-C_{hs})^2),$$
M
$$h^{(k-1)}(0) = h_{k-1} = B_1 H_1^{(k-1)}(0) + B_2 H_2^{(k-1)}(0) + ... + B_s H_s^{(k-1)}(0).$$
M

In the same way when $x = L$, we have:

$$
\begin{aligned}
&g(L)=g_{L0}=A_1\sin(\varepsilon_g^2(L-C_{g1})^2)+A_2\sin(\varepsilon_g^2(L-C_{g2})^2)+\ldots+A_m\sin(\varepsilon_g^2(L-C_{gm})^2),\\
&g'(0)=g_{L1}=2A_1\varepsilon_g^2(L-C_{g1})\cdot\cos(\varepsilon_g^2(L-C_{g1})^2)+2A_2\varepsilon_g^2(L-C_{g2})\cos(\varepsilon_g^2(L-C_{g2})^2)+\ldots\\
&+2A_m\varepsilon_g^2(L-C_{gm})\cos(\varepsilon_g^2(L-C_{gm})^2),\\
&\text{M}\\
&\text{M}\\
&g^{(j-1)}(L)=g_{L(j-1)}=A_1G_1^{(j-1)}(L)+A_2G_2^{(j-1)}(L)+\ldots+A_mG_m^{(j-1)}(L).
\end{aligned}
\tag{7}
$$

$$
\begin{aligned}
&h(L)=h_{L0}=B_1\sin(\varepsilon_h^2(L-C_{h1})^2)+B_2\sin(\varepsilon_h^2(L-C_{h2})^2)+\ldots+B_s\sin(\varepsilon_h^2(L-C_{hs})^2),\\
&h'(L)=h_{L1}=2B_1\varepsilon_h^2(L-C_{h1})\cdot\cos(\varepsilon_h^2(L-C_{h1})^2)+2B_2\varepsilon_h^2(L-C_{h2})\cos(\varepsilon_h^2(L-C_{h2})^2)+\ldots\\
&+2B_s\varepsilon_h^2(L-C_{hs})\cos(\varepsilon_h^2(L-C_{hs})^2),\\
&\text{M}\\
&h^{(k-1)}(L)=h_{L(k-1)}=B_1H_1^{(k-1)}(L)+B_2H_2^{(k-1)}(L)+\ldots+B_sH_s^{(k-1)}(L).\\
&\text{M}
\end{aligned}
$$

By replacing Eq. (5) in Eq. (1), we can obtain the following:

$$
\begin{aligned}
&DE_1: f_1\left(A_1G_1(x)+\ldots+A_mG_m(x),A_1G_1'(x)+\ldots+A_mG_m'(x),B_1H_1(x)+\ldots+B_sG_s(x),\ldots\right),\\
&DE_2: f_2\left(A_1G_1(x)+\ldots+A_mG_m(x),A_1G_1'(x)+\ldots+A_mG_m'(x),B_1H_1(x)+\ldots+B_sG_s(x),\ldots\right),\\
&\vdots\\
&DE_n: f_n\left(A_1G_1(x)+\ldots+A_mG_m(x),A_1G_1'(x)+\ldots+A_mG_m'(x),B_1H_1(x)+\ldots+B_sG_s(x),\ldots\right).
\end{aligned}
\tag{8}
$$

Each sentence of Eq. (8) is correct in every x in domain, like $x=0$ or $x=L$, so:

$$
\begin{aligned}
&DE_1(0): f_1\left(A_1G_1(0)+\ldots+A_mG_m(0),A_1G_1'(0)+\ldots+A_mG_m'(0),B_1H_1(0)+\ldots+B_sG_s(0),\ldots\right),\\
&DE_1(L): f_1\left(A_1G_1(L)+\ldots+A_mG_m(L),A_1G_1'(L)+\ldots+A_mG_m'(L),B_1H_1(L)+\ldots+B_sG_s(L),\ldots\right),\\
&DE_2(0): f_2\left(A_1G_1(0)+\ldots+A_mG_m(0),A_1G_1'(0)+\ldots+A_mG_m'(0),B_1H_1(0)+\ldots+B_sG_s(0),\ldots\right),\\
&DE_2(L): f_2\left(A_1G_1(L)+\ldots+A_mG_m(L),A_1G_1'(L)+\ldots+A_mG_m'(L),B_1H_1(L)+\ldots+B_sG_s(L),\ldots\right),\\
&\vdots\\
&DE_n(0): \left(A_1G_1(0)+\ldots+A_mG_m(0),A_1G_1'(0)+\ldots+A_mG_m'(0),B_1H_1(0)+\ldots+B_sG_s(0),\ldots\right),\\
&DE_n(L): f_n\left(A_1G_1(L)+\ldots+A_mG_m(L),A_1G_1'(L)+\ldots+A_mG_m'(L),B_1H_1(L)+\ldots+B_sG_s(L),\ldots\right).
\end{aligned}
\tag{9}
$$

When we have $m+s$ sentences in Eq. (3), the initial or boundary conditions in Eqs. (6)–(7) and (9) make $(k-1)+(j-1)+2n$ sentences. If the following inequality is correct, we have more unknown coefficients than sentences, so it is not possible to determine the radial basis function coefficients.

$$m+s>k+j+2n-2. \tag{10}$$

So, we differentiate Eq.(9) in the initial or boundary condition points to add more sentences to the problem in order to indicate the desired coefficients:

$$\begin{aligned}
&DE_1' : f_1'\Big(g(x), g'(x), ..., g^{(j)}(x), h(x), h'(x), ..., h^{(k)}(x), ...\Big),\\
&DE_2' : f_2'\Big(g(x), g'(x), ..., g^{(j)}(x), h(x), h'(x), ..., h^{(k)}(x), ...\Big),\\
&\vdots\\
&DE_n' : f_n'\Big(g(x), g'(x), ..., g^{(j)}(x), h(x), h'(x), ..., h^{(k)}(x), ...\Big).
\end{aligned} \tag{11}$$

Furthermore, if that was not enough, we differentiate the Eq. (11) one more time and continue to do so until all $A_1, ..., A_m, B_1, \dots B_s$ coefficients can be found.

$$\begin{aligned}
&DE_1'' : f_1''\Big(g(x), g'(x), ..., g^{(j)}(x), h(x), h'(x), ..., h^{(k)}(x), ...\Big),\\
&DE_2'' : f_2''\Big(g(x), g'(x), ..., g^{(j)}(x), h(x), h'(x), ..., h^{(k)}(x), ...\Big),\\
&\vdots\\
&DE_n'' : f_n''\Big(g(x), g'(x), ..., g^{(j)}(x), h(x), h'(x), ..., h^{(k)}(x), ...\Big).
\end{aligned} \tag{12}$$

In the last step, we solve the system of unknowns resulting from Eqs. (6)–(7), (9) and maybe Eqs. (11)–(12) and compute the coefficients; consequently, the ultimate answer of $g(x)$ and $h(x)$ is built. It should be mentioned that coefficients are correct for specific problem parameters, and we should redo some parts of the process for new ones.

3. Result and Discussion

In this section, we solved four vibration problems with various physics via the new trigonometric radial basis function based on the previous section's procedure. All problems have a second-order nonlinear ordinary differential equation and are initial value problems. Each problem was solved for different conditions, and plots for displacement or rotation were extracted. Furthermore, to determine the NTRBF method's accuracy, we calculated the cumulative and maximum errors with the contribution of the numerical 4th-order Runge-Kutta method and presented it in figures and tables.

3.1. Example I: Circular Sector Oscillator

The first problem is a nonlinear differential equation of a sectorial oscillator solved by the Global Residue Harmonic Balance Method (GRHBM) [31]. The oscillator is solid and homogenous, and there is no surface friction. The radius (R) and angle (α) of the sector should be indicated to solve the problem. Fig. 1 shows a schematic of the oscillator.

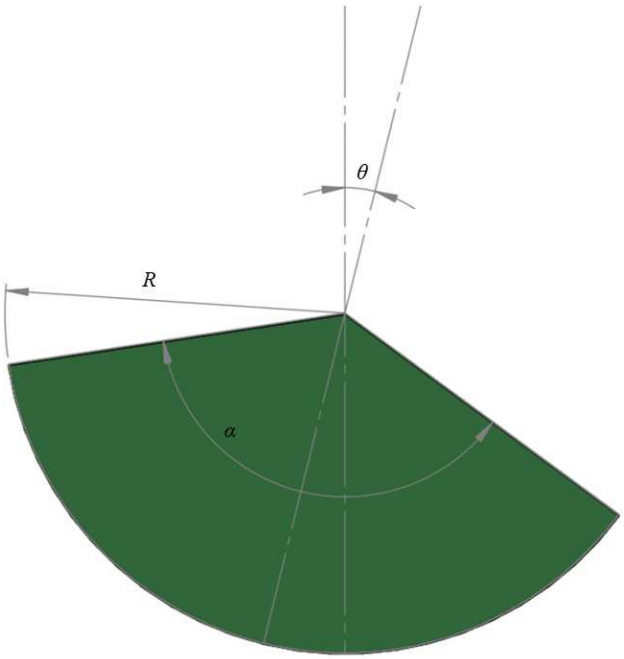

Fig. 2 Schematic figure of the circular sector oscillator

The main equation and initial conditions for oscillation are as follows:

$$\left(\frac{3}{2}R^2-\frac{4\sin(\alpha)}{3\alpha}R\cos(\theta)\right)\ddot{\theta}+R\left(\frac{3R\sin(\alpha)}{3\alpha}\sin(\theta)\right)\dot{\theta}^2+\frac{2\sin(\alpha)}{3\alpha}g\sin(\theta)=0, \tag{13}$$

$$\theta(0)=A, \qquad \dot{\theta}(0)=0, \tag{14}$$

We introduce $\bar{y}$ the center of mass and λ a dimensionless parameter:

$$\bar{y}=\frac{2R\sin\alpha}{3\alpha}, \quad \lambda=\frac{\bar{y}}{R}, \tag{15}$$

By using the mentioned parameters, Eq. (13) transforms to:

$$\Theta:\ddot{\theta}+10\delta(12-\theta^2)\theta^2\ddot{\theta}+\delta(\theta^4-20\theta^2+120)\theta\dot{\theta}^2+\mu\theta-20\beta\theta^3+\beta\theta^5=0, \tag{16}$$

Where η,δ,β, and μ are (g is the acceleration of gravity for all problems):

$$\eta=\frac{3}{2\lambda}-\frac{2}{R},\delta=\frac{1}{120\eta},\beta=\frac{\mu}{120},\mu=\frac{g\lambda}{R\eta}. \tag{17}$$

The reference study solved the Eq. (16) by GRHBM for several problem conditions and compared the results with the Modified Homotopy Perturbation Method (MHPM) and the classic numerical Runge-Kutta method. The outcomes show the excellent accuracy of GRHBM compared to MHPM; however, we applied the NTRBF to the problem. As a sample of the solution, the corresponding centers and shape parameters for the problem are as follows:

$$\begin{aligned}&\varepsilon=0.177,\\&C_1=0.9028,\\&C_2=1,\\&C_3=2,\\&C_4=3.321.\end{aligned} \tag{18}$$

If we consider four sentences in the series of $\theta(t)$, we have:

$$\begin{aligned}&\theta(t)=A_1\sin(0.177^2(t-0.9028)^2)+A_2\sin(0.177^2(t-1)^2)+\\&A_3\sin(0.177^2(t-2)^2)+A_4\sin(0.177^2(t-3.321)^2)\end{aligned} \tag{19}$$

The expanded form of Eq. (19) is:

$$\begin{aligned}&\theta(t)=A_1\sin(0.177t-0.1597956)^2+A_2\sin(0.177t-0.177)^2+\\&A_3\sin(0.177t-0.354)^2+A_4\sin(0.177t-0.587817)^2.\end{aligned} \tag{20}$$

Regarding the number of sentences in Eq. (20), we need four boundary conditions to determine the unknowns. For $\alpha=\pi/3$, $R=15$, and $A=\pi/6$, the boundary conditions are as follows (BC4 is achieved by differentiating the Eq. (16)):

$$\begin{aligned}&\text{BC1}:\theta(0)=\text{A},\\&\text{BC2}:\dot{\theta}(0)=0,\\&\text{BC3}:\Theta(1)=0,\\&\text{BC4}:\dot{\Theta}(1)=0.\end{aligned} \tag{21}$$

Subsequently, we have:

$$\begin{aligned} &BC1: 0.02531803320A_1 + 0.03100319483A_2 + 0.1201679870A_3 + 0.3075209946A_4 = \frac{\pi}{6}, \\ &BC2: -0.05560959216A_1 - 0.06135750046A_2 - 0.1151058868A_3 - 0.1633593335A_4 = 0, \\ &BC3: \cdots \\ &BC4: \cdots \end{aligned} \tag{22}$$

By solving the system of unknowns in Eq. (22), the ultimate function of $\theta(t)$ and $\dot{\theta}(t)$ will be achieved:

$$\begin{aligned} \theta(t) = {} & 10.26989096 sin(0.177t - 0.1597956)^2 - 7.679735285 sin(0.177t - 0.177)^2 - \\ & 6.927704803 sin(0.177t - 0.354)^2 + 4.338468036 sin(0.177t - 0.587817)^2 \end{aligned} \tag{23}$$

$$\begin{aligned} \dot{\theta}(t) = {} & 3.6355414 \sin(0.177t - 0.1597956)\cos(0.177t - 0.1597956) - \\ & 2.718626291 \sin(0.177t - 0.177)\cos(0.177t - 0.177) - \\ & 2.4524075 \sin(0.177t - 0.354)\cos(0.177t - 0.354) + \\ & 1.535817685 \sin(0.177t - 0.587817)\cos(0.177t - 0.587817) \end{aligned} \tag{24}$$

Figs. 2–7 show the rotation profile in the correct time scale and error for NTRBF, and GRHBM, based on the numerical 4th-order Runge-Kutta method. As can be seen in Fig. 5, the NTRBF method error is in a symmetric form with a maximum error of -0.011750 and the cumulative error of -0.040032, and GRHBM has a maximum error of 0.026070, and the cumulative error about 0.240067 when $A = \pi / 8$. Likewise, based on Fig. 8, when $A = \pi / 6$, the utmost errors are 0.013880 and 0.120860, and the cumulative errors are -0.178994, and 0.837080 for the NTRBF method and GRHBM, respectively, which illustrates the strength of the NTRBF method due to better accuracy. At this stage, the question is whether or not another RBF can solve this problem. Among the presented RBFs in Table 1, the Poisson function is the best option to approximate, but even in that case, the most significant absolute error is about 0.2, which is a poor result. We should mention that selecting centers is limited when using the Poisson function because of the denominator's independent variable; however, it might be appropriate for vibration problems with damping.

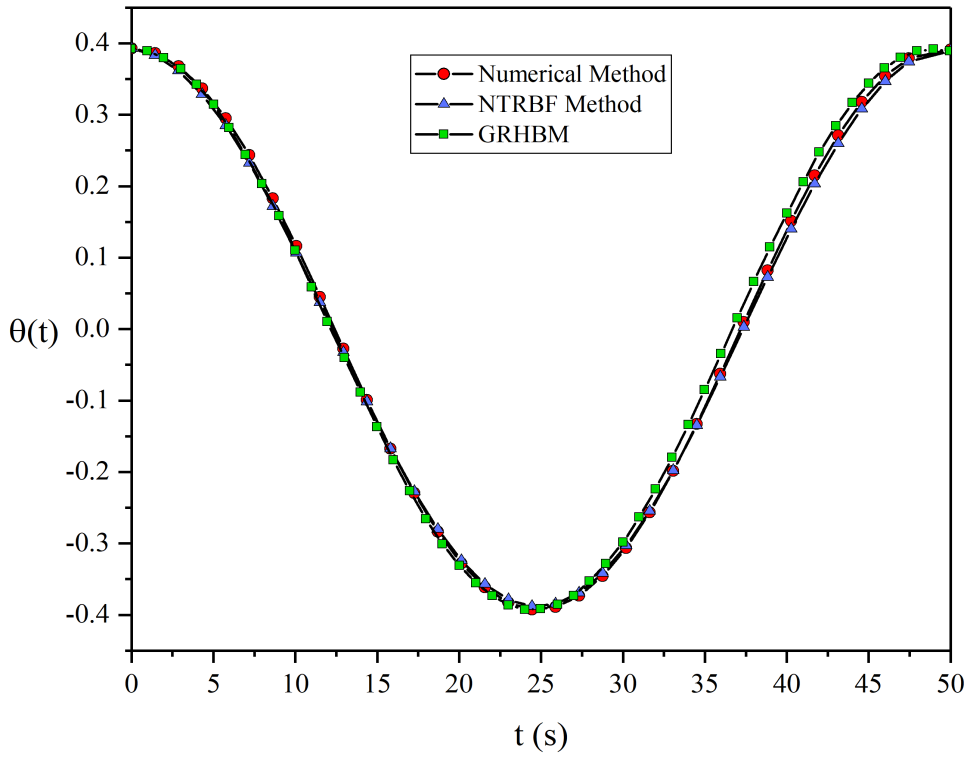

Fig. 3 Comparison of the numerical method, NTRBF method, and GRHBM, for $\theta(t)$, with $R=15$, $\alpha=\pi/3$, and $A=\pi/8$

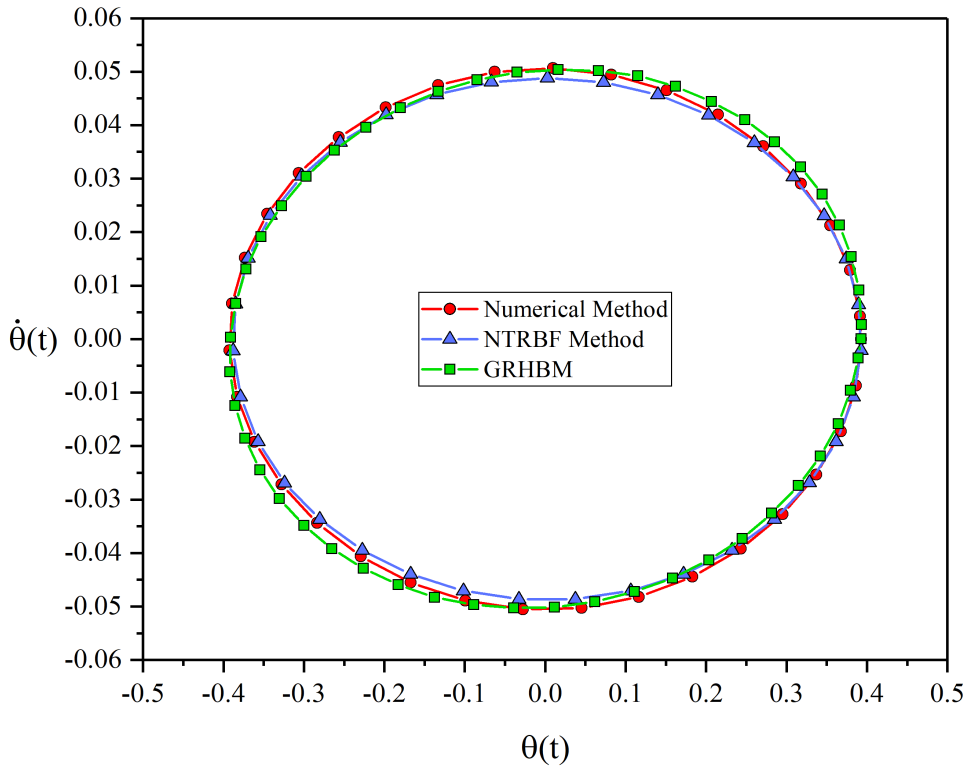

Fig. 4 Comparison of the numerical method, NTRBF method, and GRHBM, for $\dot{\theta}(t)$, with $R=15$, $\alpha=\pi/3$, and $A=\pi/8$

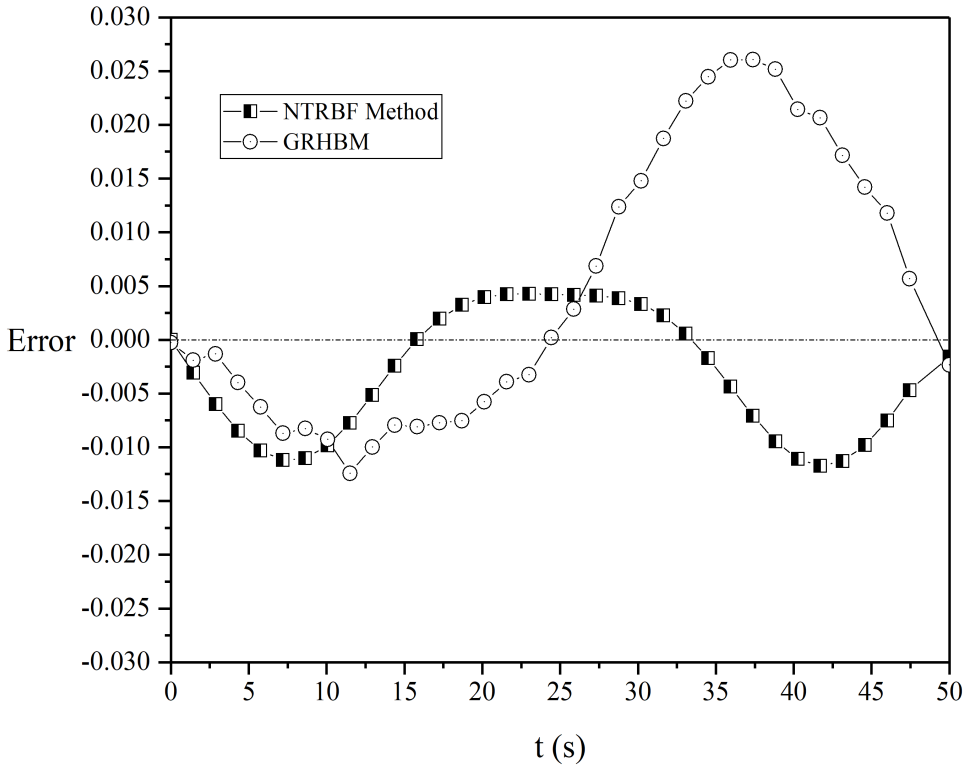

Fig. 5 Error for NTRBF method and GRHBM, with $R=15$, $\alpha=\pi/3$, and $A=\pi/8$

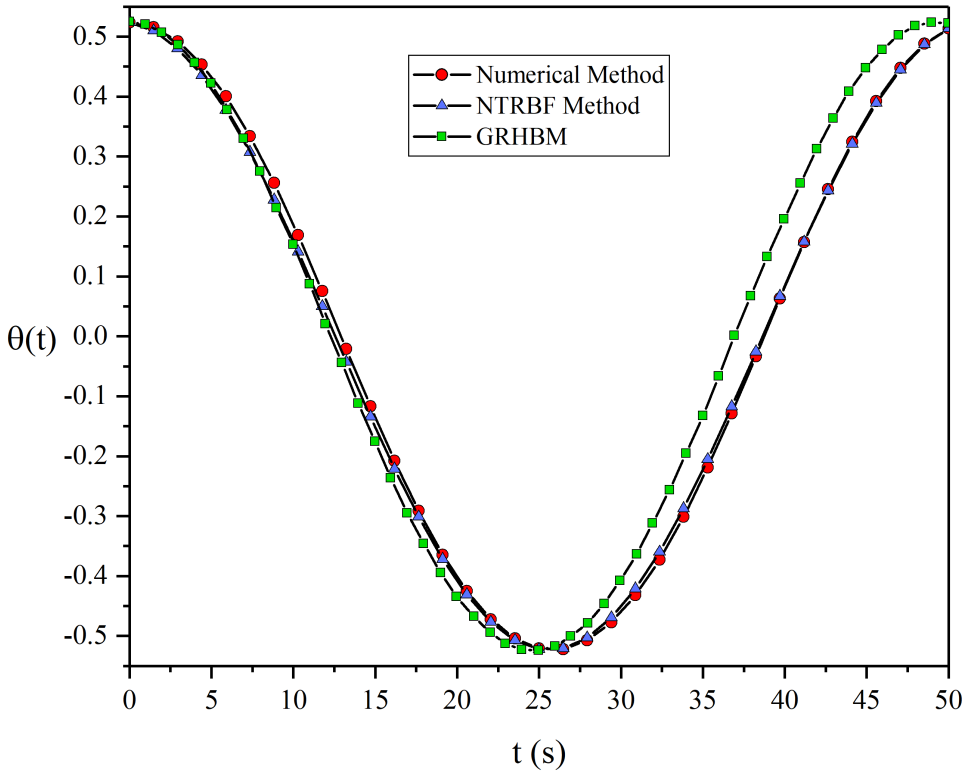

Fig. 6 Comparison of the numerical method, NTRBF method, and GRHBM, for $\theta(t)$, with $R=15$, $\alpha=\pi/3$, and $A=\pi/6$

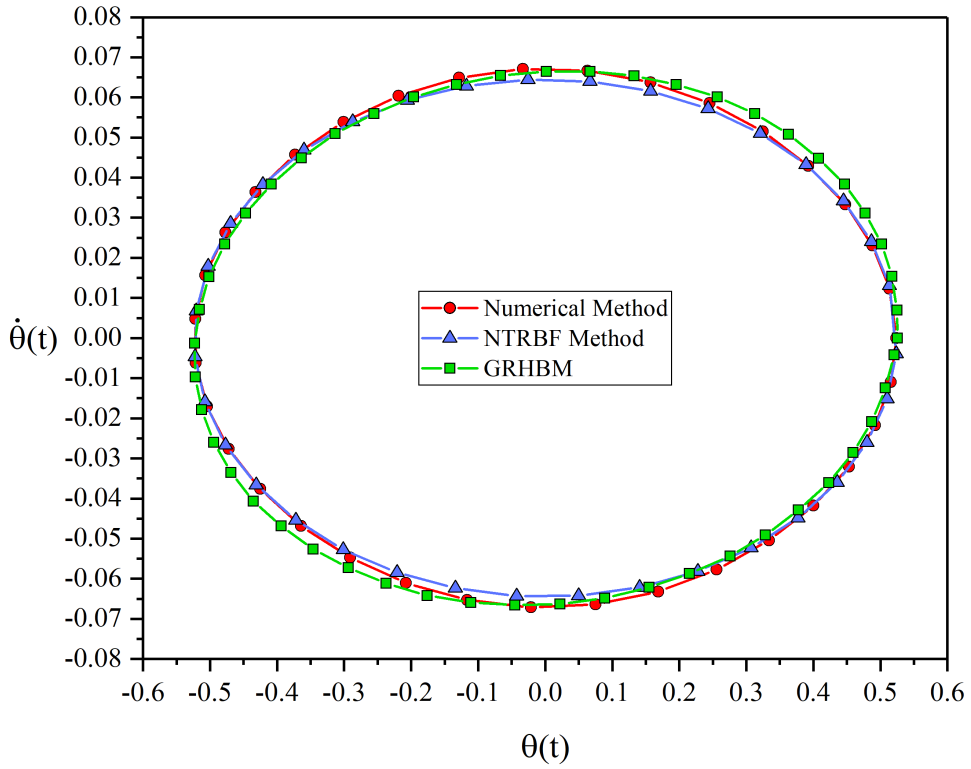

Fig. 7 Comparison of the numerical method, NTRBF method, and GRHBM, for $\dot{\theta}(t)$, with $R = 15$, $\alpha = \pi / 3$, and $A = \pi / 6$

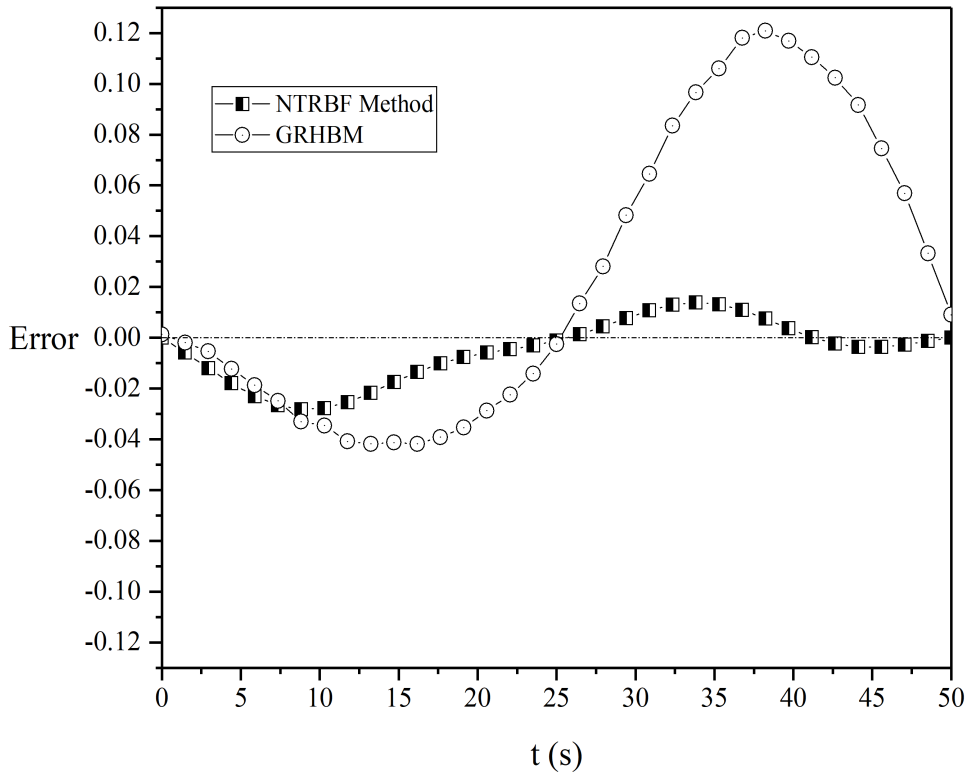

Fig. 8 Error for NTRBF method and GRHBM, with $R = 15$, $\alpha = \pi / 3$, and $A = \pi / 6$

3.2. Example II: Vibration of a Tapered Beam with non-uniform Cross-section

The second example investigates the free vibration of a tapered beam. Physical characteristics along the beam are uniform, and no energy loss is assumed. Fig. 9 shows the tapered beam related to the problem. Beam displacement as an effect of free vibration can be achieved by solving the related equation and corresponding initial conditions (Eqs. (25)–(26)) [32].

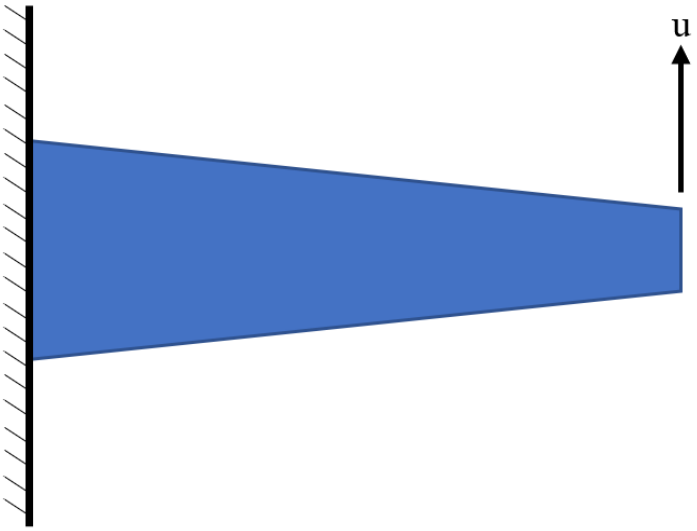

Fig. 9 Shape of a typical tapered beam

$$\ddot{u} + \frac{2\alpha u^3[3(A^2-u^2)+\beta(A^6-u^6)}{3(1+\alpha u^4)^2} + \frac{u+\beta u^5}{1+\alpha u^4} = 0, \tag{25}$$

$$u(0) = A, \quad \dot{u}(0) = 0, \tag{26}$$

In the reference paper, Eq. (25) was solved for two initial conditions by the Continuous Piecewise Linearization Method (CPLM), and the results were compared to the Linearized Harmonic Balance Method (LHBM) and RKM. The achievements of the paper show that CPLM overcomes the LHBM. As an alternative, we used NTRBF to approximate the solution. The comparison of the results with errors are shown in Figs. 10–13. The outcomes show that the maximum error for the $u(t)$ function are -0.019010, and -0.030700 for the NTRBF method, and 0.024040, and 0.051880 for CPLM, when $A = 0.5$, and $A = 1$, respectively.

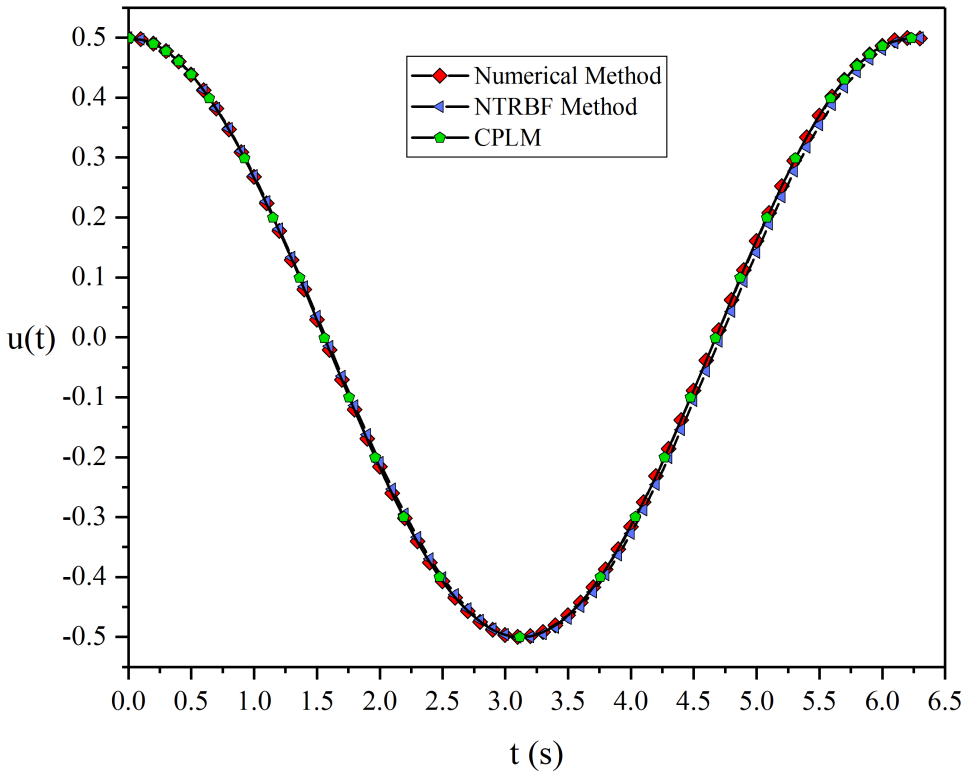

Fig. 10 Comparison of the numerical method, NTRBF method, and CPLM, for $u(t)$, with $A = 0.5$

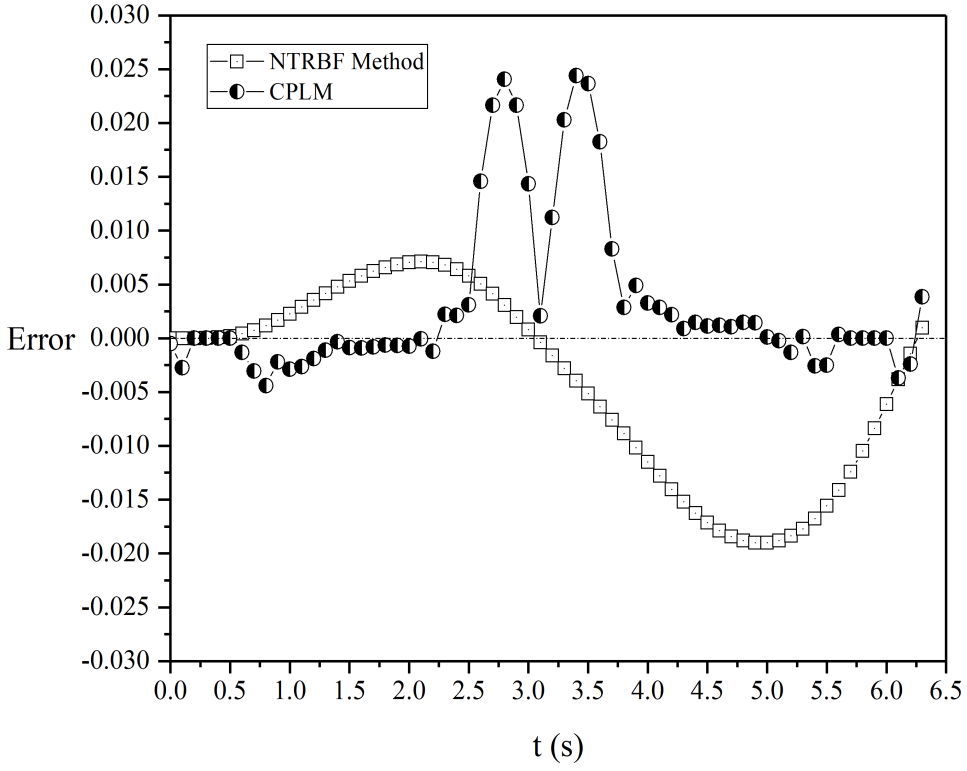

Fig. 11 Error for NTRBF method and CPLM, with $A = 0.5$

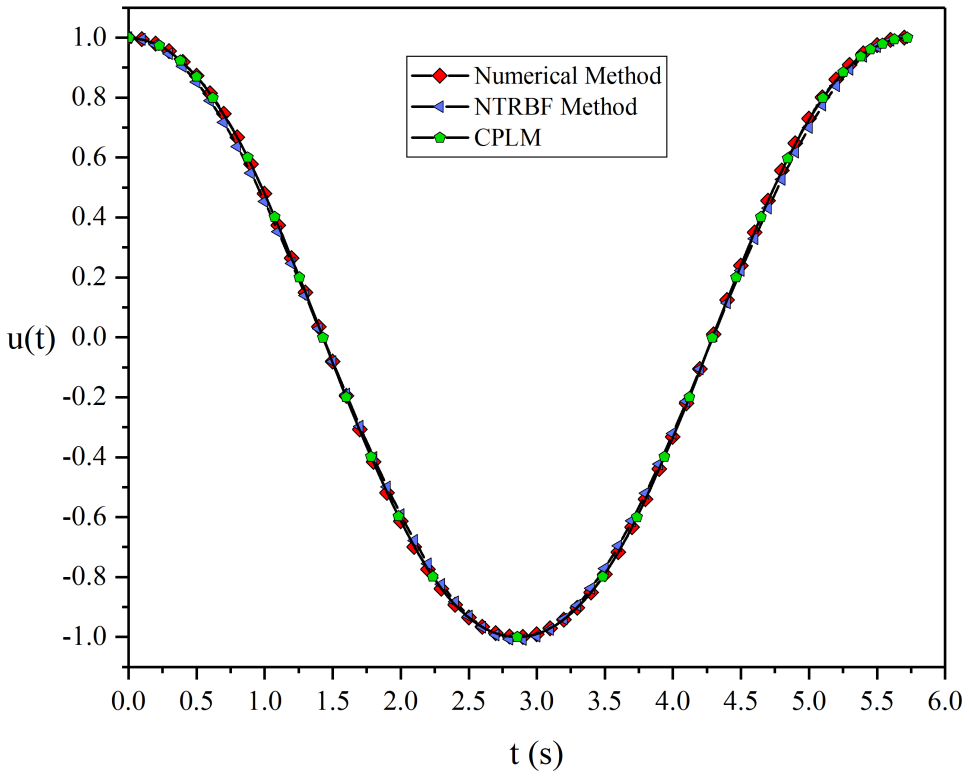

Fig. 12 Comparison of the numerical method, NTRBF method, and CPLM, for $u(t)$, with $A=1$

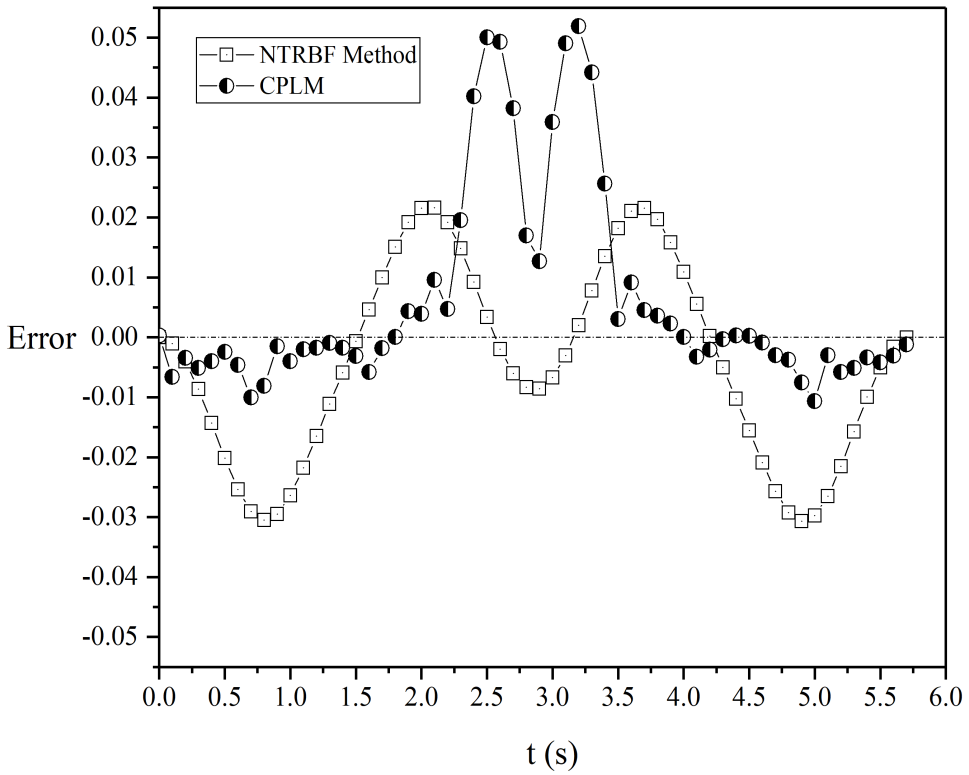

Fig. 13 Error for NTRBF method and CPLM, with $A=1$

3.3. Example III: Centrifugal Rotating Frame with an Oscillator Mass

This research considers a centrifugal rotating frame with an oscillator mass (Fig. 14). The nonlinear differential equation of the problem in Eq. (27), solved by the Differential Transform Method (DTM), Variational Iteration Method (VIM), and Homotopy Perturbation Method (HPM) [33]. One more time, the NTRBF method is applied to solve the equation for two values for A (initial condition). Outcomes are demonstrated in Figs. 15–17.

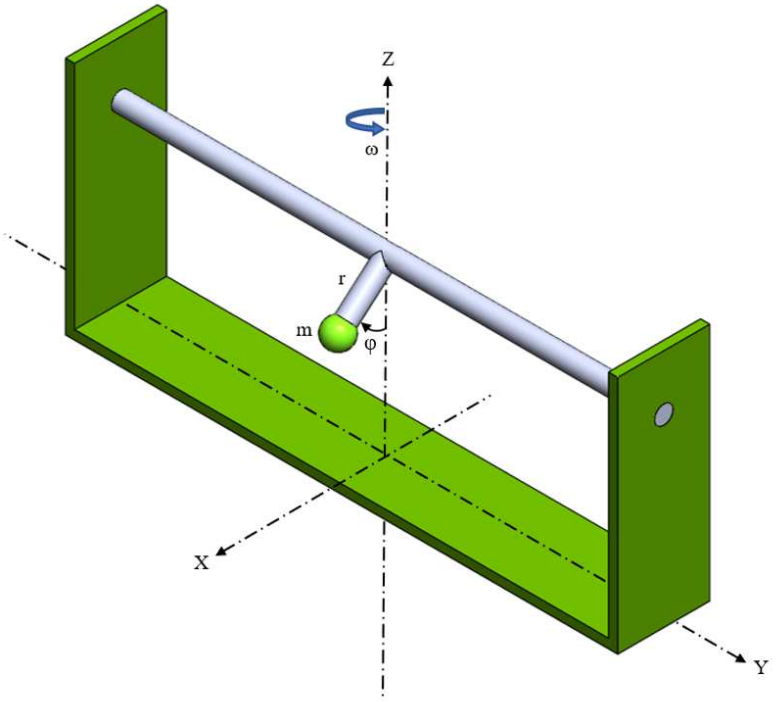

Fig. 14 Geometry of the rotating frame and oscillator mass

$$\frac{d^2\varphi}{dt^2} + (1 - \Lambda\cos\varphi)\sin\varphi = 0, \tag{27}$$

$$\varphi(0) = A, \frac{d\varphi}{dt}(0) = 0, \tag{28}$$

Where Λ is:

$$\Lambda = \frac{\omega^2 L}{g}. \tag{29}$$

Apparently, DTM and NTRBF methods perfectly match the numerical Runge-Kutta method. Nevertheless, if we look at Table 2, which presents the errors, we are able to understand that for $\Lambda = 0.25, 0.5$, and 0.75, the maximum error of $\varphi(t)$ for the NTRBF method are about -0.007080, -0.012500, and -0.013220, whereas for DTM are near 0.028440, 0.043500, and 0.023055, respectively.

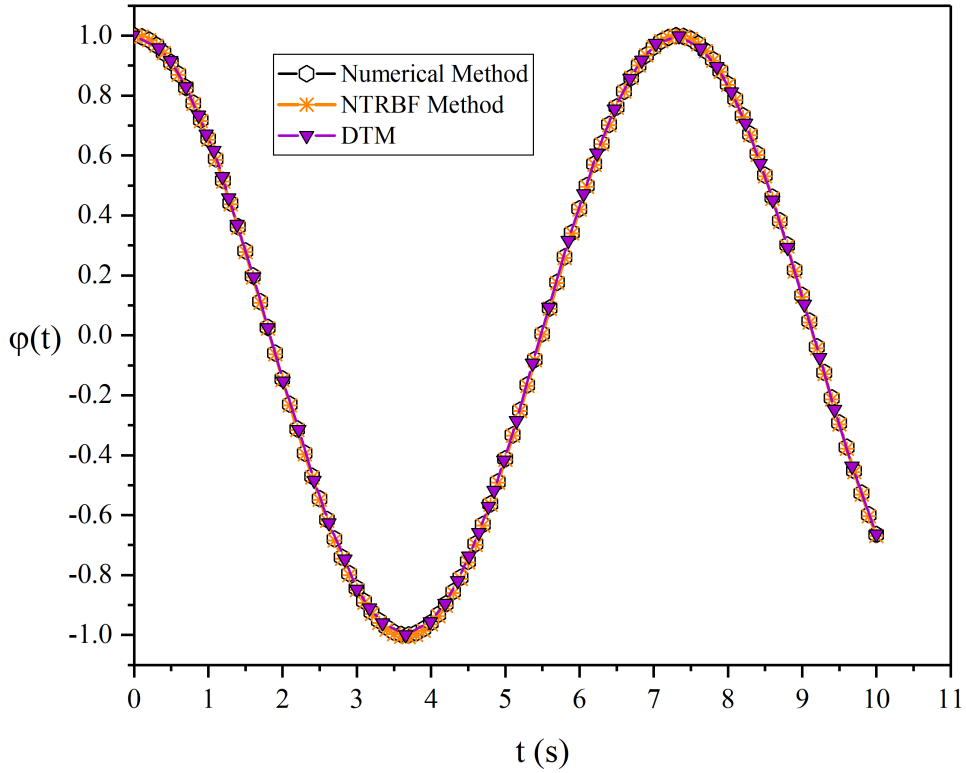

Fig. 15 Comparison of the numerical method, NTRBF method, and DTM, for $\varphi(t)$, with $\Lambda = 0.25$

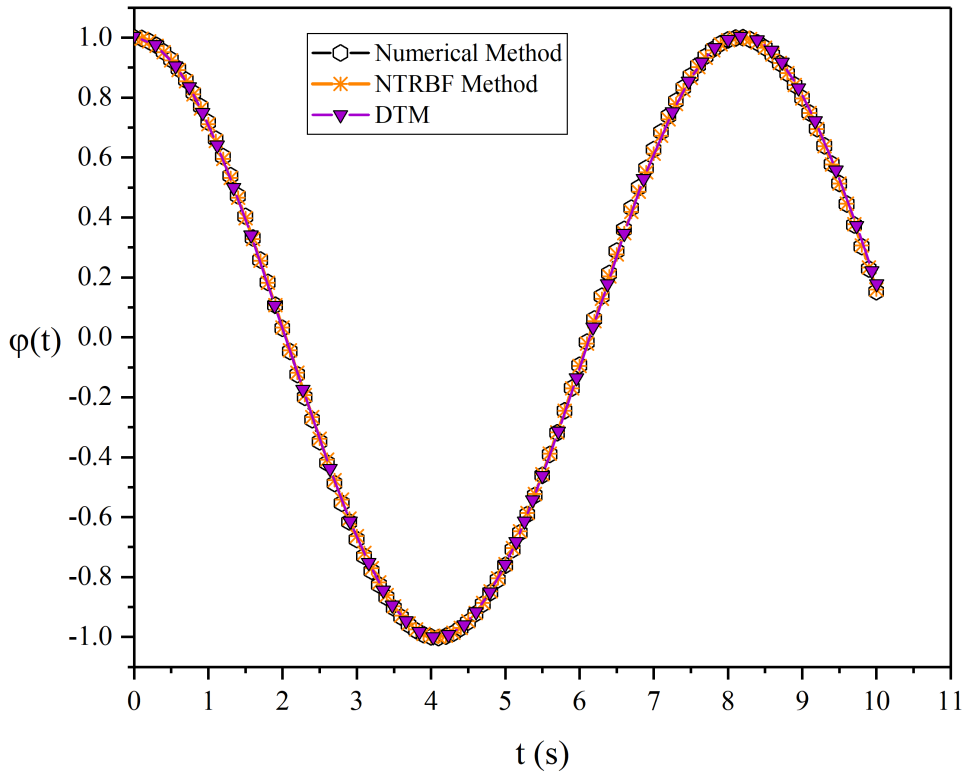

Fig. 16 Comparison of the numerical method, NTRBF method, and DTM, for $\varphi(t)$, with $\Lambda = 0.5$

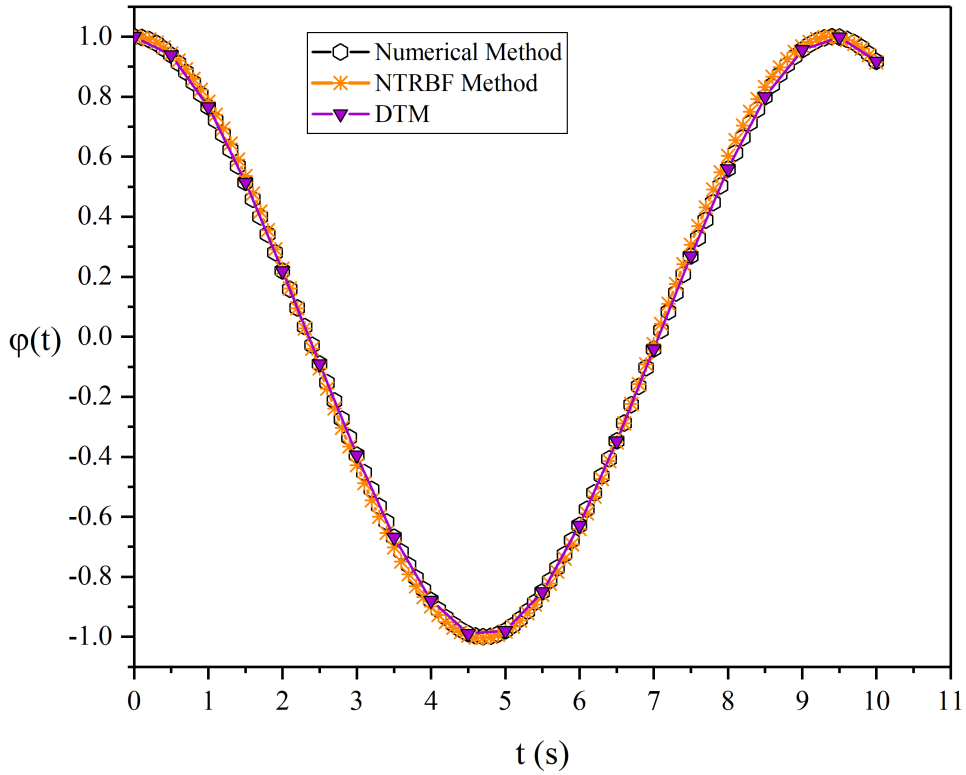

Fig. 17 Comparison of the numerical method, NTRBF method, and DTM, for $\varphi(t)$, with $\Lambda = 0.75$

Table 2 Errors for the NTRBF method and DTM

	NTRBF method	**DTM**	**NTRBF method**	**DTM**	**NTRBF method**	**DTM**
t	$\Lambda = 0.25$		$\Lambda = 0.5$		$\Lambda = 0.75$	
0.0	0.000000	-0.001250	0.000000	0.003120	0.000000	0.000000
0.5	-0.001190	0.001980	-0.002320	-0.005350	0.005770	0.001012
1.0	-0.003180	0.000635	-0.006270	-0.010110	0.016940	0.003215
1.5	-0.003960	0.000662	-0.005520	-0.010090	0.020160	0.005316
2.0	-0.003770	0.000215	0.002050	-0.002550	0.007240	0.006839
2.5	-0.004030	0.006330	0.010070	0.010610	-0.015840	0.007840
3.0	-0.005570	-0.002930	0.011260	0.011200	-0.033350	0.008308
3.5	-0.007080	0.011750	0.006420	0.003270	-0.033980	0.007943
4.0	-0.006390	0.006020	0.001930	0.002400	-0.020710	0.006228
4.5	-0.004140	0.012450	0.001960	0.004270	-0.006770	0.002464
5.0	-0.002740	0.009750	0.004700	0.003990	-0.003020	0.003666
5.5	-0.002700	0.014600	0.004140	-0.002090	-0.008960	0.010875
6.0	-0.002800	0.007190	-0.002950	-0.011000	-0.013520	0.016932
6.5	-0.001810	0.006630	-0.011380	-0.018010	-0.005140	0.020756
7.0	-0.000226	0.003170	-0.013220	-0.018670	0.016220	0.022660
7.5	-0.000342	-0.012500	-0.007810	-0.008160	0.037390	0.023055
8.0	-0.002580	-0.006180	-0.001340	0.001580	0.043500	0.021585
8.5	-0.004610	-0.009540	0.001010	0.007280	0.031380	0.017354
9.0	-0.005090	-0.006370	-0.000226	0.010090	0.011670	0.009683
9.5	-0.004850	-0.008120	0.000396	0.014900	-0.001750	0.001361
10.0	-0.005300	0.000826	0.007040	0.028440	-0.003600	0.014147

3.4. Example IV: Duffing-type Nonlinear Oscillator

In a Duffing-type oscillator, a spring's stiffness does not strictly obey Hooke's law or the damping term exists in the equation of motion. In this problem, a disk is attached to a solid hub, so as the disk rotates, the hub plays the springs roll and makes the disk oscillate (Fig. 18). Eqs.(30)–(32) are the general Duffing equation, the nonlinear equation of the problem, and the boundary conditions [34]. The problem is analyzed by Akbari-Ganji's Method (AGM).

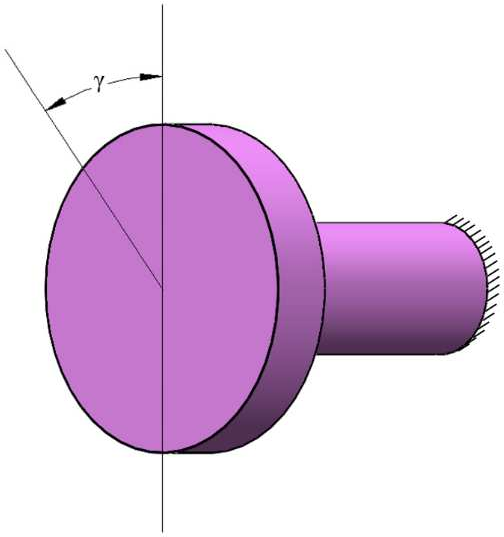

Fig. 18 Disk with the hub as a Duffing-type oscillator

$$\ddot{x}+\delta\dot{x}+\alpha x+\beta x^3=\gamma\cos(\omega t), \tag{30}$$

$$\frac{d^2}{dt^2}\gamma(t)+\frac{\gamma^3(t)}{1+\gamma^2(t)}=0, \tag{31}$$

$$\gamma(0)=A, \qquad \frac{d}{dt}\gamma(0)=0. \tag{32}$$

Figs. 19–22 demonstrate the amount of disk rotation in different conditions for initial rotation. When the disk's initial rotation is slight, the error for AGM is in the maximum state. When we increase the initial rotation from 0.01, the maximum error decreases, and when $A=10$, we have the best match for the AGM. On the contrary, the NTRBF method for all values of A has an acceptable error. Tables 3–4 show the difference between the numerical, AGM, and NTRBF methods. For AGM, we have the most significant errors about -0.023120, 0.017030, -0.02429, and -0.29491, when we have 0.01, 0.1, 1, and 10 for A, while these values for the NTRBF method are 0.000127, 0.005800, 0.04381, and 0.71387. The conclusion is that for values of initial rotation (A) more minor than 1, NTRBF has higher accuracy.

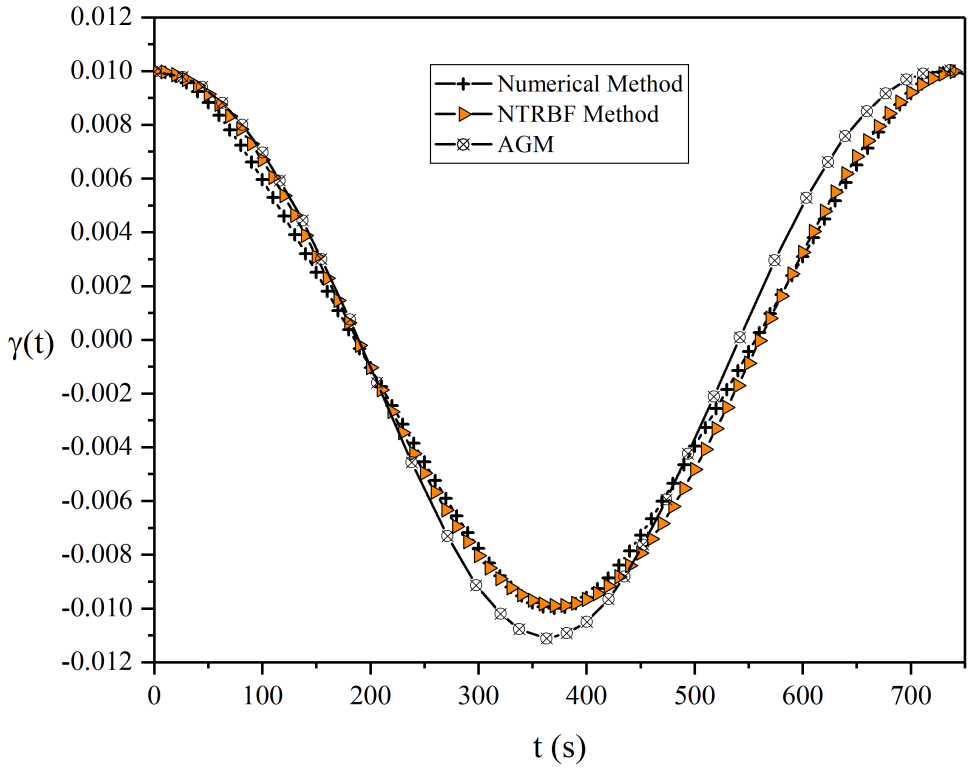

Fig. 19 Comparison of the numerical method, NTRBF method, and AGM, for $\gamma(t)$, with $A = 0.01$

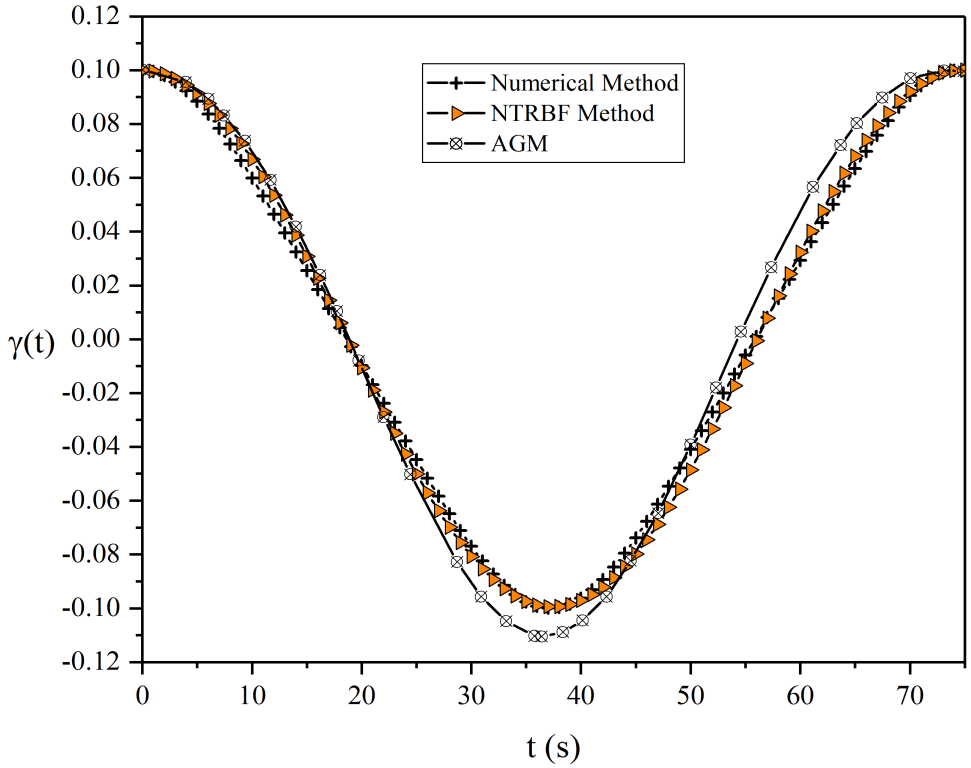

Fig. 20 Comparison of the numerical method, NTRBF method, and AGM, for $\gamma(t)$, with $A = 0.1$

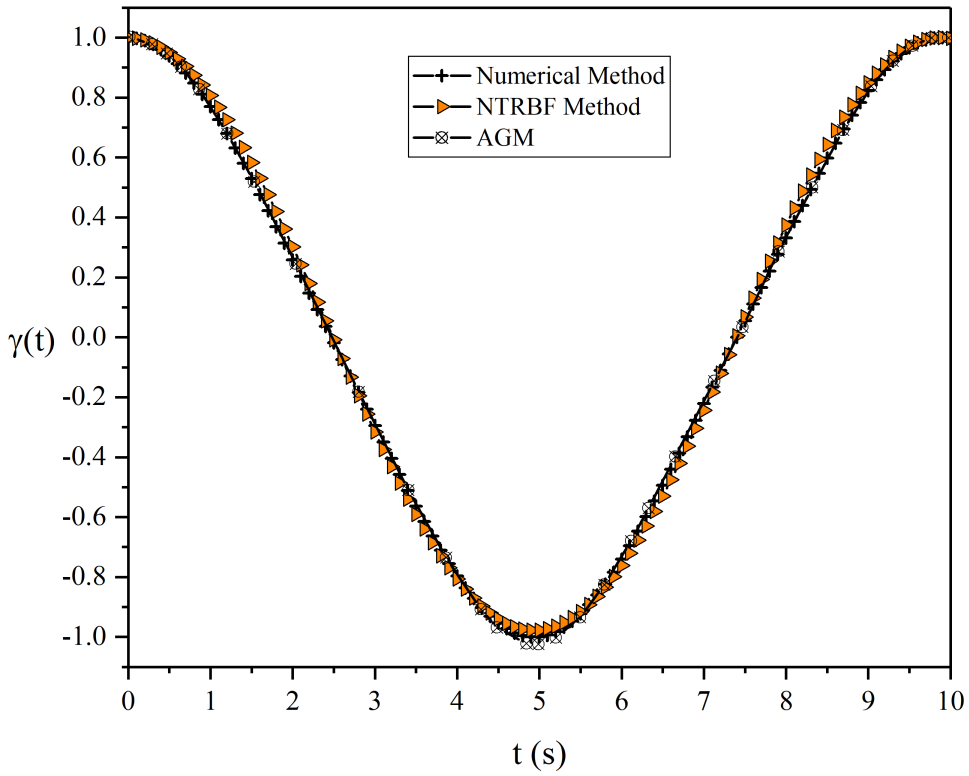

Fig. 21 Comparison of the numerical method, NTRBF method, and AGM, for $\gamma(t)$, with $A=1$

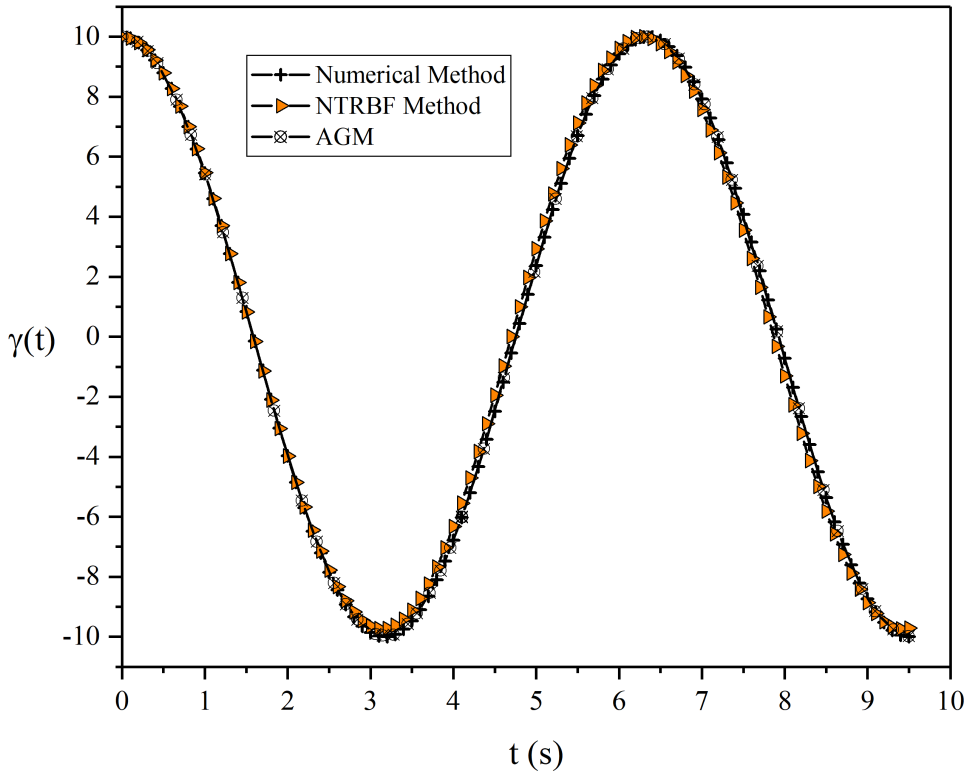

Fig. 22 Comparison of the numerical method, NTRBF method, and AGM, for $\gamma(t)$, with $A=10$

Table 3 Errors for the NTRBF method and AGM

	NTRBF method	**AGM**		**NTRBF method**	**AGM**
t	$A=0.01$		t	$A=0.1$	
0	0.000000	-0.000022	0	0.000000	0.000095
80	0.000607	-0.004220	8	0.005800	0.007810
160	0.000491	-0.012910	16	0.004270	0.006920
240	-0.0003`83	0.001740	24	-0.004810	-0.008640
320	-0.000108	0.018470	32	-0.002080	-0.012790
400	-0.000079	0.016640	40	-0.000844	-0.008640
480	-0.000863	0.008450	48	-0.007740	-0.001740
560	-0.000299	-0.001120	56	-0.001690	0.013860
640	0.000329	-0.010660	64	0.004820	0.017030
720	-0.000042	-0.018540	72	0.000195	0.001720
800	0.000127	-0.023120	80	0.001410	-0.014190

Table 4 Errors for the NTRBF method and AGM

	NTRBF method	**AGM**		**NTRBF method**	**AGM**
t	$A=1$		t	$A=10$	
0	0.00000	0.00355	0	0.00000	0.01150
1	0.03703	-0.00188	1	0.00950	-0.02367
2	0.04381	0.00635	2	-0.00987	0.04070
3	-0.02106	0.00608	3	0.21504	0.08399
4	-0.00929	0.00631	4	0.46414	0.01765
5	0.02182	-0.02429	5	0.55521	0.00597
6	-0.02048	0.00973	6	0.17619	-0.02116
7	-0.02183	0.00828	7	-0.35530	-0.00140
8	0.04231	0.00184	8	-0.58344	-0.00470

9	0.02609	-0.00127	9	-0.12855	0.02142
10	0.00149	0.00441	10	0.71387	-0.29491

4. Conclusion

The presented study proposed a novel trigonometric radial basis function for approximating vibration system nonlinear differential equations. The proposed function applied to four different problems previously solved by GRHBM, CPLM, DTM, and AGM. The results of the comparison, which prove the greater accuracy of the presented method, are as follows:

- In the circular sector oscillator, the NTRBF method has a maximum error of -0.011750, and the cumulative error is about -0.040032, whereas GRHBM has a maximum error of 0.026070, and the cumulative error about 0.240067 when $A=\pi/8$. For $A=\pi/6$, the utmost errors are 0.013880 and 0.120860, and the cumulative errors are -0.178994 and 0.837080 for the NTRBF method and the GRHBM.
- The outcomes illustrate that the maximum error for tapered beam displacement function ($u(t)$) are -0.019010 and 0.030700 for the NTRBF method and 0.024040 and 0.051880 for CPLM, when $A=0.5$, and $A=1$, respectively.
- For $\Lambda=0.25,0.5$, and 0.75, in the rotating frame, the maximum error of $\varphi(t)$ for NTRBF method are about -0.007080, -0.012500 and -0.013220, and for DTM is near 0.028440, 0.043500 and 0.023055, correspondingly.
- Considering the AGM in Duffing-type oscillator, for rotation function, we have the most significant error about -0.023120, 0.017030, -0.02429 and -0.29491, when we have 0.01, 0.1, 1, and 10 for A, while these values for the NTRBF method are 0.000127, 0.005800, 0.04381 and 0.71387. These values demonstrate that for small values of A, NTRBF has better precision, though it is relatively reverse for more than one.

Declarations

Funding: Not applicable

Conflicts of interest/Competing interests: The authors declare that they have no competing interests

Availability of data and material (data transparency): The datasets used and/or analyzed during the current study are available from the corresponding author on reasonable request

Code availability (software application or custom code): The datasets used and/or analyzed during the current study are available from the corresponding author on reasonable request

Authors' contributions: HTR proposed the novel method, analyzed the results, and worked on the code, and he created proper figures for the results and wrote the manuscript. MFN worked on the code. DDG supervised the whole process

References

1. Anjum, N., He, J.H.: Laplace transform: Making the variational iteration method easier. Appl. Math. Lett. 92, 134–138 (2019). https://doi.org/10.1016/j.aml.2019.01.016

2. Liu, C.S., Chang, C.W.: An energy regularization of the MQ-RBF method for solving the Cauchy problems of diffusion-convection-reaction equations. Commun. Nonlinear Sci. Numer. Simul. 67, 375–390 (2019). https://doi.org/10.1016/j.cnsns.2018.07.002

3. Ebrahimijahan, A., Dehghan, M., Abbaszadeh, M.: Simulation of plane elastostatic equations of anisotropic functionally graded materials by integrated radial basis function based on finite difference approach. Eng. Anal. Bound. Elem. 134, 553–570 (2022). https://doi.org/10.1016/J.ENGANABOUND.2021.10.011

4. Raja, M.A.Z., Abbas, S., Syam, M.I., Wazwaz, A.M.: Design of neuro-evolutionary model for solving nonlinear singularly perturbed boundary value problems. Appl. Soft Comput. J. 62, 373–394 (2018). https://doi.org/10.1016/j.asoc.2017.11.002

5. Kazemi, S.M.M., Dehghan, M., Foroush Bastani, A.: On a new family of radial basis functions: Mathematical analysis and applications to option pricing. J. Comput. Appl. Math. 328, 75–100 (2018). https://doi.org/10.1016/j.cam.2017.06.012

6. Oruç, Ö.: A radial basis function finite difference (RBF-FD) method for numerical simulation of interaction of high and low frequency waves: Zakharov–Rubenchik equations. Appl. Math. Comput. 394, 125787 (2021). https://doi.org/10.1016/J.AMC.2020.125787

7. Liu, C.S., Chen, W., Fu, Z.: A multiple-scale MQ-RBF for solving the inverse Cauchy

problems in arbitrary plane domain. Eng. Anal. Bound. Elem. 68, 11–16 (2016). https://doi.org/10.1016/j.enganabound.2016.02.011

8. Sun, J., Yi, H.L., Xie, M., Tan, H.P.: New implementation of local RBF meshless scheme for radiative heat transfer in participating media. Int. J. Heat Mass Transf. 95, 440–452 (2016). https://doi.org/10.1016/j.ijheatmasstransfer.2015.12.002

9. Jankowska, M.A., Karageorghis, A., Chen, C.S.: Improved Kansa RBF method for the solution of nonlinear boundary value problems. Eng. Anal. Bound. Elem. 87, 173–183 (2018). https://doi.org/10.1016/j.enganabound.2017.11.012

10. Shankar, V., Narayan, A., Kirby, R.M.: RBF-LOI: Augmenting Radial Basis Functions (RBFs) with Least Orthogonal Interpolation (LOI) for solving PDEs on surfaces. J. Comput. Phys. 373, 722–735 (2018). https://doi.org/10.1016/j.jcp.2018.07.015

11. Li, N., Su, H., Gui, D., Feng, X.: Multiquadric RBF-FD method for the convection-dominated diffusion problems base on Shishkin nodes. Int. J. Heat Mass Transf. 118, 734–745 (2018). https://doi.org/10.1016/j.ijheatmasstransfer.2017.11.011

12. Zhang, Y.: An accurate and stable RBF method for solving partial differential equations. Appl. Math. Lett. 97, 93–98 (2019). https://doi.org/10.1016/j.aml.2019.05.021

13. Bhardwaj, A., Kumar, A.: Numerical solution of time fractional tricomi-type equation by an RBF based meshless method. Eng. Anal. Bound. Elem. 118, 96–107 (2020). https://doi.org/10.1016/j.enganabound.2020.06.002

14. Reutskiy, S., Lin, J.: A RBF-based technique for 3D convection–diffusion–reaction problems in an anisotropic inhomogeneous medium. Comput. Math. with Appl. 79, 1875–1888 (2020). https://doi.org/10.1016/j.camwa.2019.10.010

15. Aràndiga, F., Donat, R., Romani, L., Rossini, M.: On the reconstruction of discontinuous functions using multiquadric RBF–WENO local interpolation techniques. Math. Comput. Simul. 176, 4–24 (2020). https://doi.org/10.1016/j.matcom.2020.01.018

16. Ullah, M.Z.: An RBF-FD sparse scheme to simulate high-dimensional Black–Scholes partial differential equations. Comput. Math. with Appl. 79, 426–439 (2020). https://doi.org/10.1016/j.camwa.2019.07.011

17. Qiao, H., Cheng, A.: A fast finite difference/RBF meshless approach for time fractional convection-diffusion equation with non-smooth solution. Eng. Anal. Bound. Elem. 125, 280–289 (2021). https://doi.org/10.1016/j.enganabound.2021.01.011

18. Mai-Duy, N., Strunin, D.: New approximations for one-dimensional 3-point and two-dimensional 5-point compact integrated RBF stencils. Eng. Anal. Bound. Elem. 125, 12–22 (2021). https://doi.org/10.1016/j.enganabound.2021.01.001

19. Ma, Z., Li, X., Chen, C.S.: Ghost point method using RBFs and polynomial basis functions. Appl. Math. Lett. 111, 106618 (2021). https://doi.org/10.1016/j.aml.2020.106618

20. Zeng, Y., Zhu, Y.: Implicit surface reconstruction based on a new interpolation/approximation radial basis function. Comput. Aided Geom. Des. 92, 102062 (2022). https://doi.org/10.1016/j.cagd.2021.102062

21. Ang, W.T.: A boundary element and radial basis function method for the Cattaneo–Vernotte equation in anisotropic media with spatially varying and temperature dependent properties. Partial Differ. Equations Appl. Math. 4, 100138 (2021). https://doi.org/10.1016/J.PADIFF.2021.100138

22. Wu, H., Han, Y., Geng, Z., Fan, J., Xu, W.: Production capacity assessment and carbon reduction of industrial processes based on novel radial basis function integrating multi-dimensional scaling. Sustain. Energy Technol. Assessments. 49, 101734 (2022). https://doi.org/10.1016/j.seta.2021.101734

23. Uddin, M., Haq, S.: RBFs approximation method for time fractional partial differential equations. Commun. Nonlinear Sci. Numer. Simul. 16, 4208–4214 (2011). https://doi.org/10.1016/j.cnsns.2011.03.021

24. Kumar, S., Piret, C.: Numerical solution of space-time fractional PDEs using RBF-QR and Chebyshev polynomials. Appl. Numer. Math. 143, 300–315 (2019). https://doi.org/10.1016/j.apnum.2019.04.012

25. Karageorghis, A., Tappoura, D., Chen, C.S.: The Kansa RBF method with auxiliary boundary centres for fourth order boundary value problems. Math. Comput. Simul. 181, 581–597 (2021). https://doi.org/10.1016/j.matcom.2020.10.010

26. Zhang, X., Yao, L., Liu, J.: Numerical study of Fisher's equation by the RBF-FD

method. Appl. Math. Lett. 120, 107195 (2021). https://doi.org/10.1016/j.aml.2021.107195

27. Tominec, I., Breznik, E.: An unfitted RBF-FD method in a least-squares setting for elliptic PDEs on complex geometries. J. Comput. Phys. 436, 110283 (2021). https://doi.org/10.1016/j.jcp.2021.110283

28. Zhao, W., Hon, Y.C., Stoll, M.: Numerical simulations of nonlocal phase-field and hyperbolic nonlocal phase-field models via localized radial basis functions-based pseudo-spectral method (LRBF-PSM). Appl. Math. Comput. 337, 514–534 (2018). https://doi.org/10.1016/J.AMC.2018.05.057

29. Fornberg, B., Larsson, E., Wright, G.: A new class of oscillatory radial basis functions. Comput. Math. with Appl. 51, 1209–1222 (2006). https://doi.org/10.1016/j.camwa.2006.04.004

30. Buhmann, M.D., Levesley, J.: Radial Basis Functions: Theory and Implementations. Math. Comput. 73, 1578–1581 (2004). https://doi.org/10.1017/CBO9780511543241

31. Lu, J., Ma, L., Sun, Y.: Analysis of the nonlinear differential equation of the circular sector oscillator by the global residue harmonic balance method. Results Phys. 19, 103403 (2020). https://doi.org/10.1016/j.rinp.2020.103403

32. Big-Alabo, A., Ossia, C.V., Ekpruke, E.O., Ogbonnia, D.C.: Large-amplitude vibration analysis of a strong nonlinear tapered beam using continuous piecewise linearization method. J. King Saud Univ. - Eng. Sci. (2020). https://doi.org/10.1016/j.jksues.2020.11.005

33. Ghafoori, S., Motevalli, M., Nejad, M.G., Shakeri, F., Ganji, D.D., Jalaal, M.: Efficiency of differential transformation method for nonlinear oscillation: Comparison with HPM and VIM. Curr. Appl. Phys. 11, 965–971 (2011). https://doi.org/10.1016/j.cap.2010.12.018

34. Mirgolbabaee, H., Ledari, S.T., Ganji, D.D.: New approach method for solving Duffing-type nonlinear oscillator. Alexandria Eng. J. 55, 1695–1702 (2016). https://doi.org/10.1016/j.aej.2016.03.007